THE JOURNAL OF PHYSICAL CHEMISTRY B

 VOLUME 107, NUMBER 45, NOVEMBER 13, 2003

LETTERS

Temperature Dependence of Hydrophobically End-Capped Poly(ethylene oxide): End Chain Effect Using ^{13}C MAS NMR

Youngil Lee,[†] Jinwoo Choi,[‡] Young-Wook Choi,[‡] and Daewon Sohn*,[‡]

Dongbu Advanced Research Institute, Daejon 305-708, Korea, and Department of Chemistry, Hanyang University, Seoul 133-791, Korea

Received: March 19, 2003; In Final Form: September 19, 2003

^{13}C magic angle spinning (MAS) NMR was used to determine the conformational change of hydrophobically end-capped poly(ethylene oxide), HEUR. The hydrophobic alkyl chains on both ends changed from trans to gauche with increasing temperature, while the poly(ethylene oxide) (PEO) main chain was either crystalline or amorphous (less-ordered crystalline) depending on temperature. The increased crystallinity due to intermolecular interaction of the PEO main chains increases the affinity of end hydrocarbons and results in a phase transition from trans to gauche form. Hydrocarbons on both ends functioned as spacers, and they increase the intermolecular spacing between the PEO main chains, where deshielding of ^{13}C signal and distinct crystalline and amorphous ^{13}C NMR peaks were observed.

Hydrophobically end-capped poly(ethylene oxide) (HEUR) is a water-soluble ABA-type polymer surfactant containing one hydrophilic poly(ethylene oxide) (PEO) middle chain and two hydrophobic end groups attached by a urethane bond.[1] In water, the poorly soluble end groups make flowerlike polymer micelles with a dense hydrophobic core surrounded by PEO chains at low concentration. The driving force for making these flowerlike micelles is the hydrophobic contacts and loop formation and chain stretching.[1−7] Recently, these polymers and their solutions in water have been examined by various experimental methods.[8−11] It has been proven that the length of the hydrophobic chain is one of the most important factors in the formation of these micelle structures.[12]

The conformational change of poly(ethylene glycol) (PEG) from crystalline and amorphous phase transitions with increasing temperature in bulk is well-known.[13] The conformational change of the *n*-alkyl chains on solid substrate has also been examined by several different methods.[14] In bulk, although it is known that the hydrophobic alkyl chains are responsible for the lower melting temperature of HEUR compared to PEG, there is a lack of information about the conformational change due to the cooperative effect between the hydrocarbons and the PEO main chain in ABA-type polymers.

The hydrophobic side chains are the predominant factors in the micellization mechanism. These were studied by comparing the thermal properties of different length *n*-alkyl chains (n = 8, 12, 18) in bulk by X-ray diffraction (XRD), differential scanning calorimetry (DSC), and ^{13}C MAS NMR.[15−18] The solid-state ^{13}C MAS NMR was mainly used to investigate the motion of the end chains and the conformational structure of HEUR at various temperatures.

Samples. Poly(ethylene glycol) (PEG, M_w = 2000 g/mol) was purchased from Fluka. The molecular weight of PEG was confirmed by mass spectroscopy, and the polydispersity was <1.05. Details of HEUR synthesis and characterizations can be found in the work by Paeng et al.[19] HEUR 2(8), HEUR 2(12), and HEUR 2(18) denote the PEO 2000 main chain with octyl,

* Corresponding author. E-mail: dsohn@hanyang.ac.kr.
[†] Dongbu Advanced Research Institute.
[‡] Hanyang University.

10.1021/jp034712y CCC: $25.00
Published on Web 10/22/2003

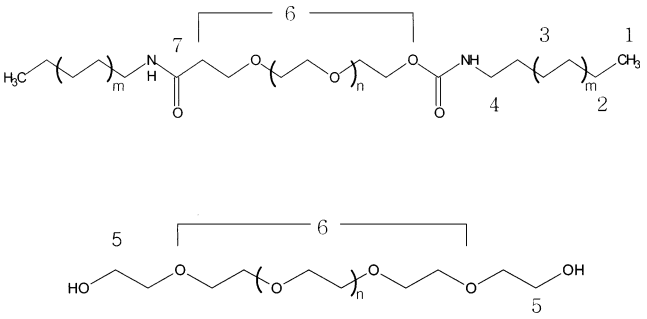

Figure 1. Chemical structure and assignment of each carbon for (a) PEG 2000 and (b) HEURs ($n = 45$; $m = 8$ for HEUR 2(8), $m = 12$ for HEUR 2(12), and $m = 18$ for HEUR 2(18)).

dodecyl, and octadecyl hydrocarbon groups on both ends, respectively. Structures and carbon assignments for PEG 2000 and the HEURs are shown in Figure 1.

Instrumentation. All ^{13}C MAS NMR spectra were obtained at the Korea Basic Science Institute (Daegu) on a Bruker DSX400 (9.4 T) to verify the conformation-dependent displacements of the molecule. High-power proton decoupling and magic angle spinning (MAS) without cross polarization (CP) were employed to determine the chemical shift variations of all carbons in the molecule as the temperature was increased.[20] The ^{13}C chemical shift was referenced to external adamantane (38.3 ppm). The continuous wave proton decoupling strength was 50 kHz. The sample was spun in a 4 mm zirconia rotor at 4 kHz at temperatures ranging from room temperature to the melting temperature of HEURs. A Bruker VT-3000 controller was used to regulate probe temperatures to ± 0.5 °C. The probe temperature readings were calibrated using $Pb(NO_3)_2$.[21] Samples were allowed to equilibrate for about 30 min at each temperature before spectral data was measured. A 36° pulse length of 2 μs for ^{13}C was used. Spin-lattice relaxation time (T_1) depends on the size of the crystalline portion.[22] If the crystalline portion is large, then T_1 will be long. However, tests showed that the intensity and shape of the crystalline line measured with repetition delays of 20 and 3 s were the same for constant number of scans and therefore represent properly the crystalline component. Spectral width and data points were 24 kHz and 8 K, respectively. A DSC from Rheometric Scientific Ltd. was used to the study the thermal properties of the HEURs. The crystallinity and the structure of HEURs were compared by XRD (Shimadzu XRD-6000). The two-dimensional wide-line separation (WISE) experiment was also performed to establish the correlation of mobility and structure of the HEURs.[23] The mobile segments in hydrocarbons were characterized with narrow ^1H line shapes. The spectrum was taken at ambient temperature on a Varian InfinityPlus 200 (4.7 T) with sample spinning frequency of 4 kHz. The mixing time, t_m, of 500 μs, 60 t_1 increments with a t_1 dwell time of 5 μs, and 1024 acquisitions were used. The pulse sequence is described in Supporting Information.

NMR spectra of PEG 2000, HEUR 2(8), HEUR 2(12), and HEUR 2(18) were obtained at room temperature and assigned as shown in Figure 2 and Table 1. It is well-known that the ^{13}C NMR spectrum of a PEG main chain at room temperature has a complicated resonance due to the presence of both amorphous and crystalline portions: an ~1 ppm upfield-shifted narrow peak for amorphous and a relatively broad peak for crystalline.[19] The amorphous portion of the random conformational structure shows a resonance at about 71 ppm.[24] The crystalline peak at about 72 ppm originates from a helical structure with a period of seven units in two turns with trans−gauche−trans for the

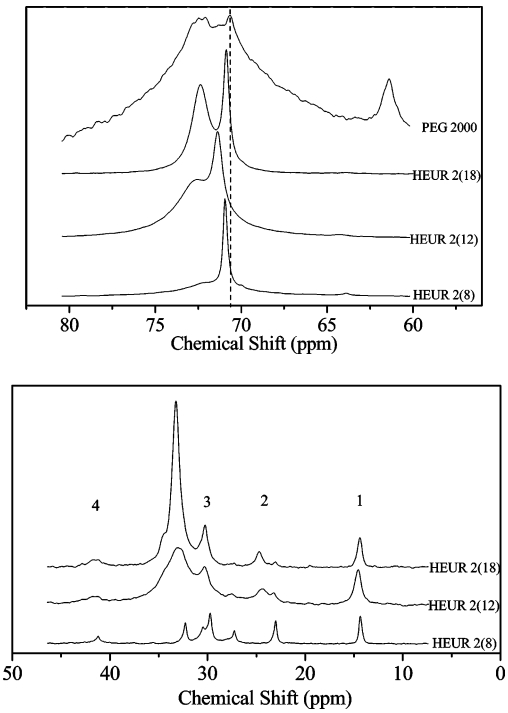

Figure 2. ^{13}C MAS NMR spectra of PEG 2000 and HEUR 2(8), 2(12), and 2(18) at room temperature.

TABLE 1: The Chemical Shift Assignment of PEG 2000 and HEUR 2(8), 2(12), and 2(18)[a]

	CO (7)	CH_3CH_2O (6)	CH_2 (5)	CH_2 (4)	$(CH_2)_n$ (3)	CH_2 (2)	CH_3 (1)
PEG 2000		72.1 (a) 70.7 (b)	61.4				
HEUR 2(18)	156.8	72.4 (a) 70.9 (b)		41.7	33.3 (c) 30.3 (d)	24.7	14.4
HEUR 2(12)	156.1	72.9 (71.3)		41.6	33.1 (c) 30.3 (d)	24.3	14.5
HEUR 2(8)	156.8	71.0		41.2	30.5 (d) 29.8	23.0	14.4

[a] Designations (a) and (b) represent the crystalline and amorphous portions on the PEG chain, respectively, and designations (c) and (d) represent the trans and mixture of trans and gauche portions on alkyl chains, respectively.

repeating unit of $-CH_2CH_2O-$. The difference in line width between these two peaks is due to differences in mobility of the PEG chains. A relatively narrow resonance of amorphous is due to the motional-averaged dipolar interactions, while the crystalline component is homogeneously broadened because of the interference between molecular motions and the proton decoupling field.[25]

On the basis of this information, the resonance at about 72 ppm in Figure 2a is the crystalline portion of the PEG main chain on HEUR, which is shown as an extremely weak resonance on HEUR 2(8). The XRD data shows sharp peaks both on HEUR 2(8) and on HEUR 2(18) as indicated in Figure 3, where the peaks of HEUR 2(18) are shifted 2° lower than those of HEUR 2(8). The XRD data shows that HEUR 2(8) has a crystalline portion. Therefore, it is possible that the two peaks at about 71 and 72 ppm in NMR measurement originated from the motional contribution due to the intermolecular spacing between the parallel aligned PEO chains rather than those from well-known mixture of crystalline and the amorphous portions. The peak at about 71 ppm represents the moving carbons on the PEO backbone. Even though it is not a true amorphous state, this is similar to what was seen for an amorphous phase. The

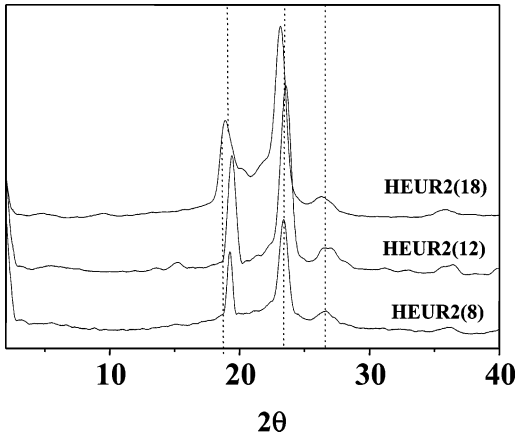

Figure 3. XRD peaks of HEUR 2(8), 2(12), and 2(18).

peak at about 72 ppm is due to the carbon signal from the crystal-like PEO backbone. Because HEUR has the hydrophobic ends on either side of PEO, crystallinity increases as the length of the hydrocarbon is increased. The short liquidlike hydrocarbon acts as a spacer and prevents intermolecular crystalline alignment of the PEO chains, especially in HEUR 2(8), which shows very weak resonance of the crystalline portion. HEUR 2(18) is easily distinguished from PEG by its two sharper peaks, which are due to increased crystallinity. Very sharp resonance of the PEO main chain indicates that no interference occurred between molecular motions and the proton decoupling. Hydrophobic intermolecular interaction of the long hydrocarbon at both ends results in the parallel alignment of PEO main chains and the increased crystallinity.

The resonance of the amorphous portion for HEUR 2(18) is slightly shifted (~0.3 ppm) downfield compared to that of the PEG 2000. This is probably due to the different intermolecular polymer chain packing in the crystal, which usually does not exceed 1 ppm.[26] In this case, the side chains of HEUR 2(18) interrupt the interpacking of PEO chains, which results in a downfield shift (i.e., toward higher chemical shift) of the resonance. This interruption, however, is not strongly affected by a small shift because the crystallinity of polymeric structure is entirely increased because of the strong intermolecular interaction of the long hydrophobic alkyl chain. For HEUR 2(12), resonances of both crystalline and moving crystalline portions are shifted more downfield and are more broadened than those of HEUR 2(18). The downfield shift is increased because of the deshielding of PEO carbons by the flexible spacer of dodecyl hydrocarbon on both ends. The spacer partially interrupts the intermolecular interaction both in the crystalline and in the moving crystalline portions of PEO chains making a less-ordered crystalline structure, which results in peak broadening. These effects are diminished in the HEUR 2(8) because of the liquidlike character of the short hydrocarbon.

Differences of molecular dynamics are discriminated by ^{1}H line shapes in the 2D WISE NMR spectrum as shown in Supporting Information. The amorphous portion having relatively high mobility shown at about 71 ppm in ^{13}C dimension leads to comparatively narrow ^{1}H line, while crystalline at about 72 ppm in ^{13}C is shown as broadened ^{1}H line. Also, gauche conformational segments of $(CH_2)_n$ units at about 30 ppm in ^{13}C dimension are relatively narrow line in the ^{1}H dimension, while the rigid trans conformational segments at about 33 ppm in ^{13}C are by the wide ^{1}H line.

The γ-gauche effect successfully accounts for the microstructural dependence of ^{13}C chemical shifts in polymers.[27] Several authors have reported that the amorphous carbons in semicrystalline polyethylene (PE) resonate 2−3 ppm upfield-shifted from the crystalline carbons.[28] These observations are expected because the crystalline carbons reside in the all-trans, planar zigzag conformation (no γ-gauche shielding), while the C−C bonds in the amorphous portions of PE possess some gauche character. It is proper for HEUR 2(18) with a longer chain to have larger hydrophobic interaction than HEUR 2(8). In particular, the resonance for the $(CH_2)_n$ units is generally observed at about 30 ppm because of alkyl chain organizations with solution-like mixtures of trans and gauche conformations.[14] Because the steric γ-gauche substituent affects the carbon shielding, $(CH_2)_n$ carbon signals at about 33 ppm can be assigned to more-ordered trans conformations as shown in Figure 2 and Table 1. The $(CH_2)_n$ units of HEUR 2(18) are observed at 33.3 ppm with a small shoulder at 30.3 ppm.[29] This corresponds to a large fraction of trans conformations and indicates a high degree of chain order in the alkyl chain, while HEUR 2(8) has a relatively strong signal at 29.8 ppm. HEUR 2(12) is similar to HEUR 2(18) except for the small contribution of the trans conformations, which are less-intense compared to those of HEUR 2(18). Pursch et al. reported that trans/gauche conformational change occurs for the surface-polymerized C30 on a silica solid surface and C18 only has gauche conformation on the silica particle.[14] The trans/gauche transition at C12 in HEUR is mainly due to the strong intermolecular interaction between PEG main chains.

The hydrophobic interaction of alkyl end chains was examined through different phases by varying the temperature. Figure 4a indicates the change of ^{13}C NMR spectra of PEG 2000 depending on experimental temperature, which was varied from room temperature up to 343 K. PEG 2000 has a rigid phase containing crystalline (72.1 ppm) and amorphous portions (70.6 ppm), which changes to a predominantly amorphous phase at 313 K. Though its melting temperature (T_m) is 325 K as observed in DSC, it has a mobile melting phase in which the amorphous phase (71 ppm) exists from 313 K. When the sample is cooled to room temperature, the crystalline phase reappears. The melting temperatures for HEUR 2(8), HEUR 2(12), and HEUR 2(18), were 316, 320, and 325 K, respectively. The NMR experiment was performed by varying the temperature of sample from room temperature to ~10 K above its T_m. For HEUR 2(8) in Figure 4b, there is no crystalline portion and the melting started at 305 K without a change of chemical shift. There is an insignificant change on splitting of the gauche contribution by temperature at ~30 ppm. Figure 4c shows the temperature dependence of HEUR 2(12), where the crystalline portion of the PEG chain disappeared and the dominant trans conformation of hydrocarbon diminished with increasing temperature. The ^{13}C NMR spectra of HEUR 2(18) are shown in Figure 4d. At 317 K, the crystalline contribution of PEG disappears and the trans conformation of hydrocarbon is diminished with an upfield shift (i.e., toward lower chemical shift). When it is cooled back to room temperature, however, the crystalline phase recovers again. As mentioned above, at 33.3 ppm, there is a chemical shift of trans zigzag conformation in crystalline hydrocarbons, and at 30.3 ppm, there are free rotating alkyl chains. In HEUR 2(18), some distinct features of ^{13}C NMR spectra are observed by side chain motions with increasing temperature: The intensity of the peak at 33.3 ppm is reduced, while the intensity at 30.3 ppm is increased. The resonance at 24.7 ppm is shifted upfield because of the thermal motion of the alkyl chain. These features are not seen in HEUR 2(8), which indicates that the alkyl chains of HEUR 2(18) are not twisted and affected by temperatures because of the high crystallinity of the long hydrocarbons.

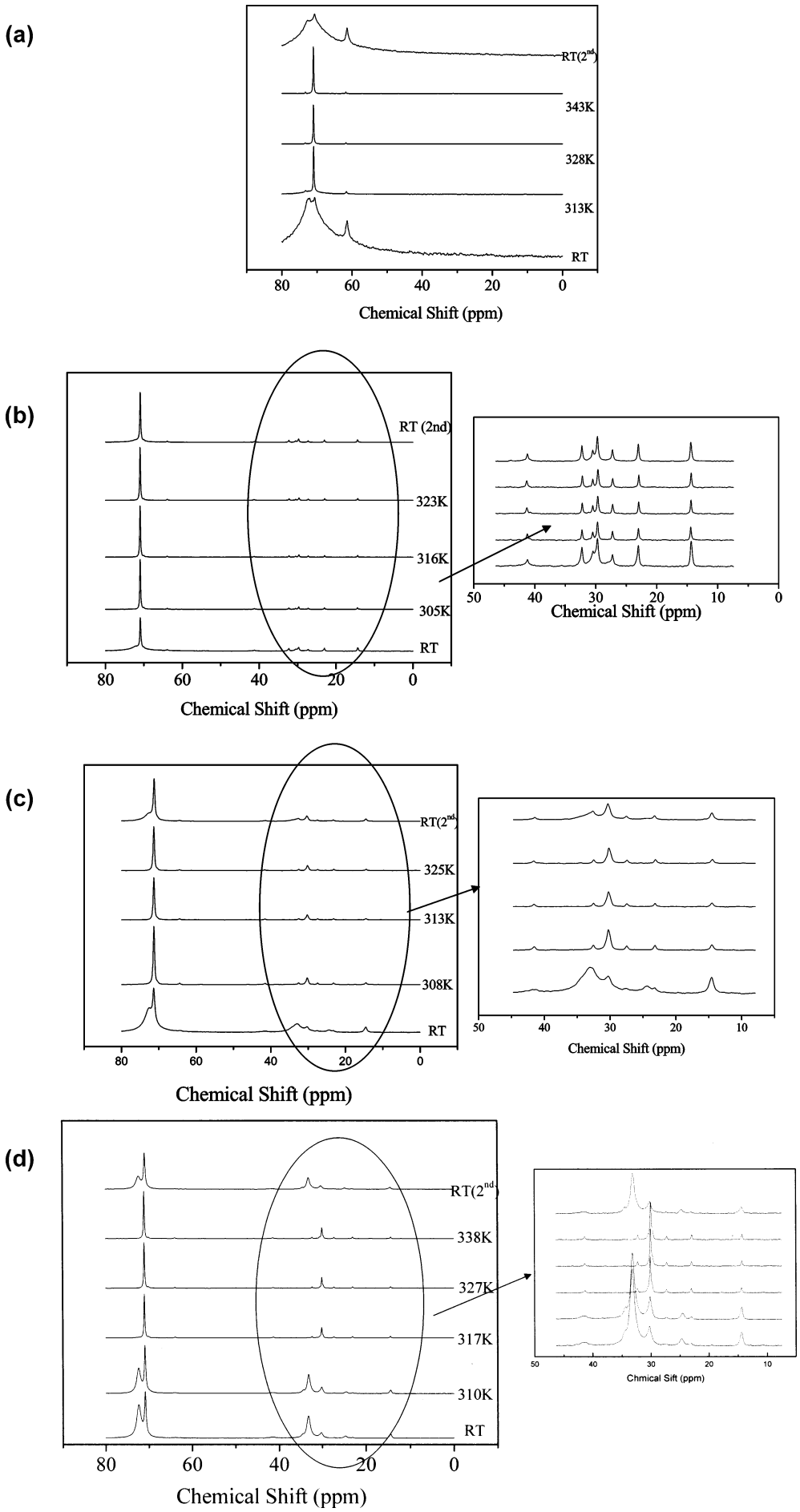

Figure 4. Temperature-dependent ^{13}C MAS NMR spectra of (a) PEG, (b) HEUR 2(8), (c) HEUR 2(12), and (d) HEUR 2(18).

In summary, the conformational change of ABA-type polymer surfactants was successfully observed in a temperature-dependent study using ^{13}C MAS NMR. The increased crystallinity due to intermolecular interaction of the PEO main chains increases the affinity of end hydrocarbons and results in a phase transition from trans to gauche form. The intermolecular distance parallel to the main chain of ABA-type polymer surfactants maintains the crystallinity and increases intermolecular spacing and segmental mobility in the PEO main chains. Hydrocarbons on both ends function like spacers, and they increase the intermolecular spacing between the PEO main chains, where we observed deshielding of ^{13}C signal and distinct crystalline and amorphous ^{13}C NMR peaks.

Acknowledgment. This work was supported by the National R & D Project for Nano Science and Technology. Y.-W. Choi is grateful for the support from KOSEF (Grant Number R-14-2002-004-01002-0). Authors gratefully acknowledge Ms. Sunha Kim, Mr. Kee Sung Han, and Korea Basic Science Institute for use of the NMR facility.

Supporting Information Available: Pulse sequence for the 2D WISE NMR experiment and 2D WISE NMR spectrum of HEUR 2(18). This material is available free of charge via the Internet at http://pubs.acs.org.

References and Notes

(1) Rao, B.; Umera, Y.; Dyke, L.; Mcdonald, P. M. *Macromolecules* **1995**, *28*, 531.
(2) Semenov, A. N.; Joanny, J. F.; Khokhlov, A. R. *Macromolecules* **1995**, *28*, 1066.
(3) Alami, E.; Abrahmsen, S. A.; Vasilescu, M.; Almgren, M. *J Colloid Interface Sci.* **1997**, *193*, 152.
(4) Lundberg, D. J.; Brown, R. G.; Glass, J. E.; Eley, R. R. *Langmuir* **1994**, *10*, 3027.
(5) Kaczmarski, J. P.; Glass, J. E. *Langmuir* **1994**, *10*, 3035.
(6) Xu, B.; Yekta, A.; Li, L.; Masoumi, Z.; Winnik, M. A. *Colloids Surf., A* **1996**, *112*, 239.
(7) Yekta, A.; Duhamel, J.; Adiwidjaja, H.; Brochard, P.; Winnik, M. A. *Langmuir* **1993**, *9*, 881.
(8) Winnik, M. A.; Yekta, A. *Curr. Opin. Colloid Interface Sci.* **1997**, *2*, 424.
(9) Francois, J.; Maitre, S.; Rawiso, M.; Sarazin, D.; Beinert, G.; Isel, F. *Colloids Surf., A* **1996**, *112*, 251.
(10) Alami, E.; Almgren, M.; Brown, W. *Macromolecules* **1996**, *29*, 2229.
(11) Tam, K. C.; Jenkins, R. D.; Winnik, M. A.; Bassett, D. R. *Macromolecules* **1998**, *31*, 4149.
(12) Paeng, K. W.; Kim, B.-S.; Kim, E.-R.; Sohn, D. *Bull. Korean Chem. Soc.* **2000**, *21*, 623.
(13) VanderHart, D. L.; Earl, W. L.; Garroway, A. N. *J. Magn. Reson.* **1981**, *44*, 361.
(14) Pursch, M.; Brindle, R.; Ellwanger, A.; Sander, L. C.; Bell, C. M.; Handel, H.; Albert, K. *Solid State Nucl. Magn. Reson.* **1997**, *9*, 191.
(15) Mathias, L. J., Ed. *Solid State NMR of Polymers*; Plenum Publishing Corporation: New York, 1991.
(16) Sanders, J. K. M.; Hunter, B. K. *Modern NMR Spectroscopy*; Oxford University Press: Oxford, U.K. 1987.
(17) Günter, H. *NMR Spectroscopy*; John Wiley & Sons: New York, 1990.
(18) Bovey, F. A.; Mirau, P. A. *NMR of Polymers*; Academic Press: San Diego, CA, 1996.
(19) Paeng, K.; Choi, J.; Park, Y.; Sohn, D. *Colloids Surf., A* **2003**, *220*, 1.
(20) Wagner, G. W.; Yang, Y. *J. Mol. Struct.* **1999**, *479*, 93.
(21) Mildner, T.; Ernst, H.; Freude, D. *Solid State Nucl. Magn. Reson.* **1995**, *5*, 269.
(22) Schantz, S. *Macromolecules* **1997**, *30*, 1449.
(23) Schmidt-Rohr, K.; Clauss, J.; Spiess, H.-W. *Macromolecules* **1992**, *25*, 3273.
(24) Johansson, A.; Tegenfeldt, J. *Macromolecules* **1992**, *25*, 4712.
(25) Dechter, J. J. *J. Polym. Sci., Polym. Lett. Ed.* **1985**, *23*, 261.
(26) Spěváček, L.; Paternostre, J.; Damman, A.; Draye, C.; Dosière, M. *Macromolecules* **1998**, *31*, 3612.
(27) Earl, W. L.; VanderHart, D. L. *Macromolecules* **1979**, *12*, 762.
(28) Bunn, A.; Cudby, M. E. A.; Harris, R. K.; Packer, K. J.; Say, B. J. *Polymer* **1982**, *23* (5), 694.
(29) (a) Pursch, M.; Strohschein, S.; Händel, H.; Albert, K. *Anal. Chem.* **1986**, *68*, 386. (b) Albert, K.; Händel, H.; Pursch, M.; Strohschein, S.; Pesek, J. J.; Matyska, M. T.; Abuelafyya, R. R. *Chemically Modified Surfaces*; Royal Chemical Society: Cambridge, U.K., 1996; Vol. 6, p 30.